Published by Institute of Physics Publishing for SISSA

Received: *July 11, 2008*
Revised: *August 2, 2008*
Accepted: *September 12, 2008*
Published: *September 17, 2008*

JHEP09(2008)080

Computation of the string tension in three dimensional Yang-Mills theory using large N reduction

Joe Kiskis

Department of Physics, University of California,
Davis, CA 95616, U.S.A.
E-mail: jekiskis@ucdavis.edu

Rajamani Narayanan

Department of Physics, Florida International University,
Miami, FL 33199, U.S.A.
E-mail: rajamani.narayanan@fiu.edu

Abstract: We numerically compute the string tension in the large N limit of three dimensional Yang-Mills theory using Wilson loops. Space-time loops are formed as products of smeared space-like links and unsmeared time-like links. We use continuum reduction and both unfolded and folded Wilson loops in the analysis.

Keywords: Lattice Gauge Field Theories, 1/N Expansion.

Contents

JHEP09(2008)080

1. Introduction

The method of large N continuum reduction [1, 2] for SU(N) gauge theory allows for the calculation of the infinite volume, infinite N limit of certain physical quantities using volumes reduced to a small physical size. Numerical estimates [1, 2] of the physical critical size above which continuum reduction holds indicate that this method can be used to produce practical results. The chiral condensate [3] and the pion decay constant [4] were calculated in the large N limit in four dimensions using continuum reduction. In this paper, we show that the method can be extended beyond bulk quantities and that it also produces reliable results for quantities with space-time dependence such as the heavy quark potential, from which the string tension can be extracted.

A precise calculation of the string tension in three dimensional SU(N) gauge theories has been performed with N up to 8 on large lattices [5]. In this paper, we present a complementary calculation with $N = 47$ on 5^3 lattices using continuum reduction. The calculation of ref. [5] used correlation functions of smeared Polyakov loops to extract the string tension. After extrapolating to $N = \infty$ and to the continuum, the result was

$$\frac{\sqrt{\sigma}}{g^2 N} = 0.1975 \pm 0.0002 - 0.0005 \tag{1.1}$$

where g is the gauge coupling. This has to be compared with the analytical calculation in [6], namely, $\frac{1}{\sqrt{8\pi}} \approx 0.1995$. Although the two results are not in perfect agreement, the main observation is that the approximations used in the analytical calculation are very well motivated.

The string tension for SU(N) as per the analytical calculation [6] is

$$\sigma = \frac{g^2 c_A}{2\pi}\frac{g^2 c_F}{2} = \left[g^2 N\right]^2 \frac{1}{8\pi}\left[1 - \frac{1}{N^2}\right]. \tag{1.2}$$

c_A and c_F are the quadratic Casimirs in the adjoint and fundamental representation, respectively. The mass parameter $\frac{g^2 c_A}{2\pi}$ naturally enters the analytical calculation, and the second factor $\frac{g^2 c_F}{2}$ arises from the Wilson loop operator in the fundamental representation.

The numerical computation in [5] shows that the agreement gets better as one gets closer to $N = \infty$. Like the analytical result, the numerical result also shows a correction from $N = \infty$ that goes like $\frac{1}{N^2}$, but the coefficient of $\frac{1}{N^2}$ is not the same for the numerical and the analytical computations.

Since the numerical and the analytical results are close to each other even for $N = 2$ (less than 4%), we can use the analytical formula to get a feel for the finite N corrections to the infinite N result. Therefore, we expect the finite N corrections to be smaller than the error in Eqn(1.1) if $N > 32$.

In this paper, we use continuum reduction [1, 2] to directly compute the $N = \infty$ limit of the string tension by working at large enough N so that the finite N corrections are smaller than the numerical errors. We find that

$$\frac{\sqrt{\sigma}}{g^2 N} = 0.1964 \pm 0.0009 \tag{1.3}$$

This result and that of (1.1) are consistent at the level of their one sigma errors. This level of agreement is, in turn, consistent with neither the large N extrapolation of ref. [5] nor the volume reduction of the present calculation having unexpected errors. While both of the numerical results lie below the analytical estimate, the discrepancy is relatively small. Thus the numerical evidence that the analytical result is an excellent first approximation that captures much of the physics remains strong.

The paper is organized as follows. We explain how we use smeared Wilson loops to compute the string tension in section 2. The lattice results for the string tension along with the continuum extrapolation are also presented in this section. An intermediate step in our calculation is the dimensionless ground state string energy $m(k)$. In section 3, we show results for $m(k)$ at one fixed lattice coupling to illustrate its behavior as a function of k and how it is used to extract the string tension. We also show that $m(k)$ is unaffected by the smearing parameter. We illustrate the extraction of $m(k)$ at one fixed coupling in section 4. Here we show how the smearing parameter affects the overlap with the ground state. The main result in this paper is obtained using $N = 47$. We show that the finite N and finite volume corrections are small at this value of N in section 5. We explain why this method is preferred over the Creutz ratio in section 6.

2. String tension using Wilson loops and continuum reduction

Consider SU(N) Yang-Mills theory on a periodic lattice with the standard Wilson gauge action. The method of [5] is to measure the string tension using correlations of Polyakov

JHEP09(2008)080

loops with separation t that wind around a space direction. Continuum reduction [1, 2] implies that the large N Yang-Mills theory in a continuum box of size l^3 is independent of l as long as $l > l_c = 1/T_c$ with T_c being the deconfining temperature. One should be able to compute expectation values of Wilson loops of arbitrary size on an l^3 continuum box using folded Wilson loops and extract the string tension. To implement this approach to the three-dimensional Yang-Mills theory string tension, we use the following procedure:

- We fix the lattice size to L^3. We use $L = 5$ for the most part and only use $L = 4$ to verify reduction.
- We fix N so that finite N corrections are small. We set $N = 47$ and show using one instance that finite N corrections are small at $N = 47$.
- We pick an appropriate range of lattice coupling $b = \frac{1}{g^2 N}$.
  - b cannot be too small since we have to be away from the bulk transition on the lattice associated with the development of gap in the eigenvalue distribution of the plaquette operator [10]. Therefore, we pick $b \geq 0.6$.
  - b cannot be too big since we have to be below the deconfining transition for $L = 5$. Therefore, we pick $b \leq 0.8$ [11].
- We use smeared space-like links and unsmeared time-like links.
- We use the tadpole improved coupling $b_I = be(b)$ to set the scale and consider $K \times T$ Wilson loops $W(K,T)$ with $1.5 < \frac{K}{b_I}, \frac{T}{b_I} < 12.5$. This amounts to expectation values of Wilson loops that range from 0.82 to $2 \cdot 10^{-4}$.
- Keeping K fixed, we fit
$$lnW(k,t) = -a - m(k)t; \tag{2.1}$$
where $k = \frac{K}{b_I}$ and $t = \frac{T}{b_I}$ are the dimensionless extent in the space and time direction respectively. $m(k)$ is the dimensionless ground state energy. This fit assumes that there is a perfect overlap with the ground state. Note that a should be zero since $W(k,0) = 1$. Any small deviation from zero seen in the fit is due to the contribution from excited states. This can be seen by noting that $W(k,t)$ should behave as $e^{-a}e^{-m(k)t} + (1 - e^{-a})e^{-m_1(k)t}$ with $m_1(k) > m(k)$. Then, $lnW(k,t) = -a - m(k)t + ln\left[1 + (e^a - 1)\, e^{-[m_1(k)-m(k)]t}\right]$. The last term is numerically insignificant in the range of t being considered.
- Finally, $m(k)$ is fit to $\sigma b_I^2 k + c_0 b_I + \frac{c_1}{k}$. The combination $\sqrt{\sigma} b_I$ is plotted as a function of b_I^{-2}. We expect lattice spacing effects to lead off as b_I^{-2} in Yang-Mills theories and this is indeed the case in figure 1. The continuum limit extracted from this figure was quoted in eq. (1.3).

The use of smeared links improves the measurement of Wilson loops. They enhance the overlap of the space-like sides of the Wilson loops with the ground state. This increases the signal relative to the fluctuations and simplifies the t behavior of the loops [7]. One

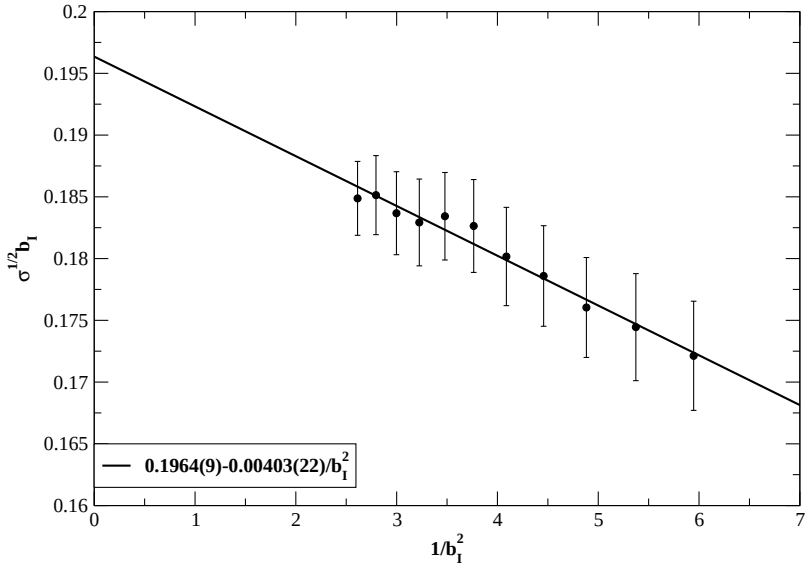

Figure 1: The string tension is plotted as a function of the lattice spacing b_I^{-1}. The fit is an extrapolation to the continuum.

step in the iteration takes one from a set $U_k^{(i)}(x_1, x_2, t)$ to a set $U_k^{(i+1)}(x_1, x_2, t)$, by the following equation:

$$
\begin{aligned}
X_1^{(i+1)}(x_1,x_2,t) &= (1-f)U_1^{(i)}(x) + \frac{f}{2}U_2^{(i)}(x_1,x_2,t)U_1^{(i)}(x_1,x_2+1,t)\left[U_2^{(i)}(x_1+1,x_2,t)\right]^\dagger \\
&\quad + \frac{f}{2}\left[U_2^{(i)}(x_1,x_2-1,t)\right]^\dagger U_1^{(i)}(x_1,x_2-1,t)U_2^{(i)}(x_1+1,x_2-1,t) \\
X_2^{(i+1)}(x_1,x_2,t) &= (1-f)U_2^{(i)}(x) \\
&\quad + \frac{f}{2}U_1^{(i)}(x_1,x_2,t)U_2^{(i)}(x_1+1,x_2,t)\left[U_1^{(i)}(x_1,x_2+1,t)\right]^\dagger \\
&\quad + \frac{f}{2}\left[U_1^{(i)}(x_1-1,x_2,t)\right]^\dagger U_2^{(i)}(x_1-1,x_2,t)U_1^{(i)}(x_1-1,x_2+1,t) \\
U_k^{(i+1)}(x_1,x_2,t) &= X_k^{(i+1)}(x_1,x_2,t)\frac{1}{\sqrt{[X_k^{(i+1)}(x_1,x_2,t)]^\dagger X_k^{(i+1)}(x_1,x_2,t)}}; \quad k=1,2
\end{aligned}
\tag{2.2}
$$

Note that time-like links, $U_3(x_1, x_2, t)$, are not smeared. Also note that smearing only involves space-like staples. There are two parameters, namely, the smearing factor f and the number of smearing steps n. Only the product $\tau = fn$ matters, and f plays the role of a discrete smearing step. For a given τ, the overlap of the smeared loop with the ground state does not depend on f as long as it is small. But the overlap of the smeared loop with the ground state does depend upon τ. We set the value of the smearing parameter to $\tau = 2.5$ by choosing $f = 0.1$ and $n = 25$. To study the effect of varying τ, we also consider $\tau = 1.25$ ($f = 0.05$ and $n = 25$) at one coupling.

3. Extraction of string tension

SU(N) gauge fields were generated on a 5^3 periodic lattice using the standard Wilson action.

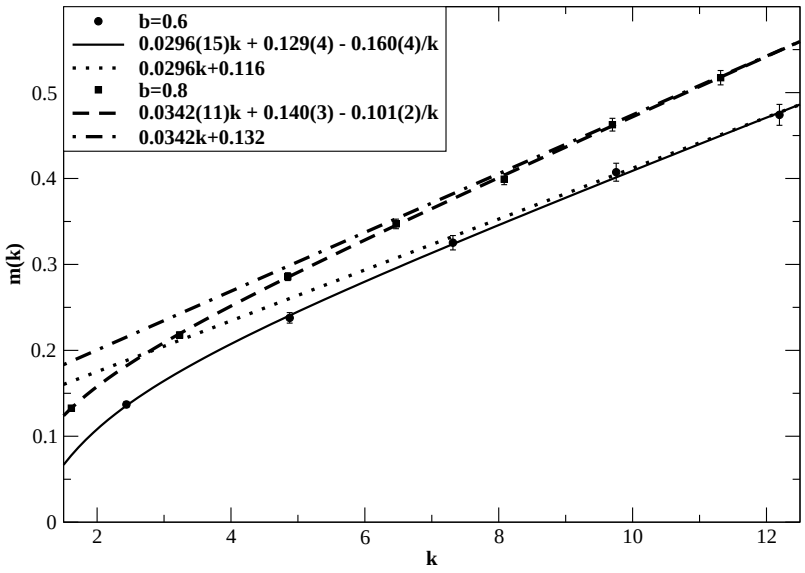

Figure 2: The ground state energy $m(k)$ as a function of k for the coarse and fine lattice spacings considered here.

One gauge field update of the whole lattice [2] is one Cabibbo-Marinari heat-bath update of the whole lattice followed by one SU(N) over-relaxation update of the whole lattice. A total of 1500 such updates were used to achieve thermalization. Measurements were separated by 10 such updates and all estimates are from a total of 832 such measurements. Errors in all quantities at a fixed b and N were obtained by jackknife with single elimination.

The ground state energy $m(k)$ obtained as a function of $k = \frac{K}{b_I}$ is fit to

$$m(k) = \sigma b_I^2 k + c_0 b_I + \frac{c_1}{k} \tag{3.1}$$

We expect σb_I^2 to approach a finite value in the continuum limit ($b_I \to \infty$). The same is expected for c_1. For large, unsmeared or symmetrically smeared Wilson loops with $t \gg k$, the universal value is $-\frac{\pi}{24} \approx -0.13$ [8] rather than the value $-\frac{\pi}{6}$ for Polyakov loops [9] that was seen in [5]. The $c_0 b_I$ term is present due to the perimeter divergent contribution, and therefore it is expected to logarithmically diverge in the continuum limit. Since, we do not smear the time-like gauge fields, the divergence in this term is not tamed.

The method will encounter difficulties in extracting the physically relevant string tension from eq. (3.1) if $c_0 b_I$ is large. However, because we do not go to very weak couplings, we see in figure 2 that $c_0 b_I$ is not too large. It is not necessary to go to weaker couplings since the string tension computed at the couplings we have chosen can be used to get a good estimate of the string tension in the continuum limit as is evident in figure 1.

The three parameter fit of $m(k)$ as a function of k is shown in figure 2. The fit has two degrees of freedom at the coarse lattice spacing of $b = 0.6$ and has four degrees of freedom at the fine lattice spacing of $b = 0.8$. As mentioned before, errors in σb_I^2, c_1, and $c_0 b_I$ are obtained by jackknife with single elimination. Unlike the estimate of the leading coefficient σb_I^2, the estimates of the sub-leading ones are not as reliable. Consider the *dotted* line

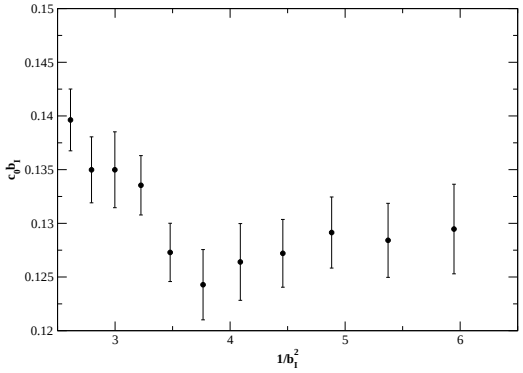

Figure 3: The behavior of the coefficient $c_0 b_I$ in the fit of $m(k)$ vs k is consistent with the presence of a $\ln b_I$ term due to the perimeter divergence.

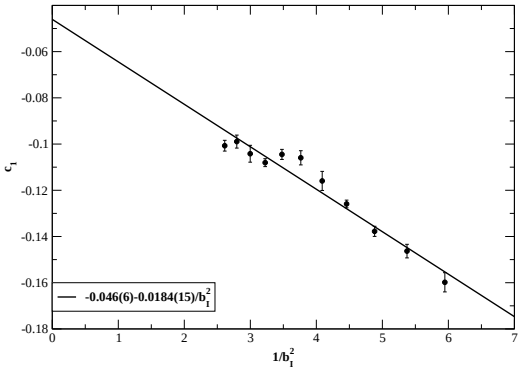

Figure 4: The behavior of the coefficient c_1 in the fit of $m(k)$ vs k shows the existence of a continuum limit.

and *dot-dashed* line in figure 2. The constant term in each of these lines is obtained by evaluating $c_0 b_I + c_1/k$ at $k = 12.5$. The coefficient of the linear term in each is set to the same value as the one in the full three parameter fit. A comparison of the *dotted* line with the *solid* line and a comparison of the *dot-dashed* line with the *dashed* line shows that the $1/k$ term becomes relevant only if $k < 7$. There are only two data points at $b = 0.6$ and three data points at $b = 0.8$ where the $1/k$ effect is significant. As such, we do not expect our estimate of c_1 and $c_0 b_I$ to be as reliable as the estimate of σb_I^2.

The behaviors of $c_0 b_I$ and c_1 as a function of b_I^{-2} are shown in figure 3 and figure 4. Between these two terms, $c_0 b_I$ is the dominant one. The rise in $c_0 b_I$ at smaller b_I^{-2} is consistent with the presence of a $\ln b_I$ term from a perimeter divergence. The estimate of c_1 is least reliable since it is dominated by the other two terms in the fit of $m(k)$ as a function of k. A fit of c_1 as shown in figure 4 is consistent with the existence of a continuum limit. One should note that the number of degrees of freedom in the three parameter fit of $m(k)$ increases as b_I decreases and this will have an effect in the determination of the sub-leading terms. We believe this is reason the fit of c_1 versus b_I does not pass through all the data points. Since we do space-like but not time-like smearing and since our loops do not generally have $t \gg k$, it not surprising to see a result that disagrees with the universal value but has the same sign and order of magnitude.

4. Extraction of $m(k)$

The dimensionless ground state energy $m(k)$ is extracted at a fixed k by fitting $\ln W(k,t)$ to $-a - m(k)t$ as discussed in section 2. While $m(k)$ should be independent of the smearing parameter $\tau = fn$, the value of a is expected to depend τ.

We will use $b = 0.8$ as the coupling to illustrate the extraction of $m(k)$. Figure 5 and figure 6 show the performance of the fit for two different values of τ, namely, 2.5 and 1.25 respectively. The *solid circles* show the data points without errors. The *solid lines* show the fit of the data. Seven values of t were used to fit the data at one k, and data at seven different values of k were fitted. This amounted to all Wilson loops from 1×1 to 7×7

JHEP09(2008)080

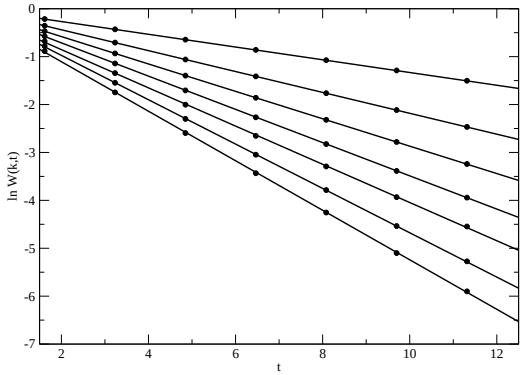

Figure 5: Plot of $\ln W(k,t)$ as a function of t for seven different values of k at $b = 0.8$ with $\tau = 2.5$.

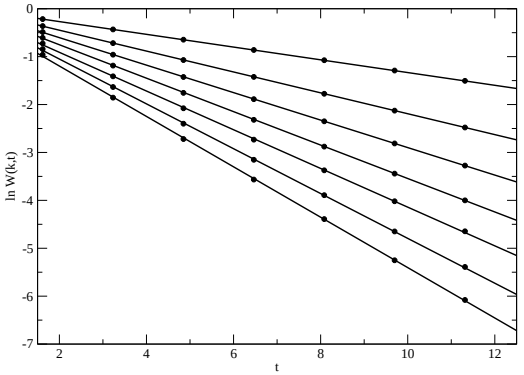

Figure 6: Plot of $\ln W(k,t)$ as a function of t for seven different values of k at $b = 0.8$ with $\tau = 1.25$.

k	1.62	3.23	4.85	6.47	8.08	9.70	11.31
a	0.001	0.003	0.009	0.019	0.055	0.047	0.071
$m(k)$	0.133	0.218	0.286	0.347	0.399	0.464	0.517

Table 1: Fit parameters corresponding to the fit $\ln W(k,t) = -a - m(k)t$ for seven different values of k at $b = 0.8$ with $\tau = 2.5$.

k	1.62	3.23	4.85	6.47	8.08	9.70	11.31
a	0.002	0.012	0.029	0.054	0.102	0.114	0.144
$m(k)$	0.133	0.218	0.287	0.349	0.404	0.468	0.526

Table 2: Fit parameters corresponding to the fit $\ln W(k,t) = -a - m(k)t$ for seven different values of k at $b = 0.8$ with $\tau = 1.25$.

on the 5^3 lattice. The set of thermalized configurations used at $\tau = 2.5$ is statistically independent from the set used at $\tau = 1.25$. The fit parameters are shown in table 1 and table 2. Only the average values of the fit parameters are listed.

Investigation of table 1 and table 2 shows that $m(k)$ does not depend on τ. There is a small difference in the two values of $m(k)$ at a fixed k for the two different values of τ if k is large. But figure 7 shows that this difference is within errors. Furthermore, the fitted values of σb_I^2 for the two different values of τ are the same within errors.

The values of a in table 1 and table 2 do show a variation with τ and k. Since a smaller value of τ implies less smearing, the overlap with the ground state is less for smaller τ, and this results in a larger value of a at smaller τ. The value of a is very close to zero for small k indicating excellent overlap with the ground state for the chosen value of τ. As k increases, the length of the loop increases and the perimeter divergence has a stronger effect. This results in a larger value of a as k increases at a fixed τ.

5. Finite N effects

Two issues need to be addressed with the analysis performed so far. We have fixed our value of N assuming finite N effects are small. If N is not large enough, finite N effects need to

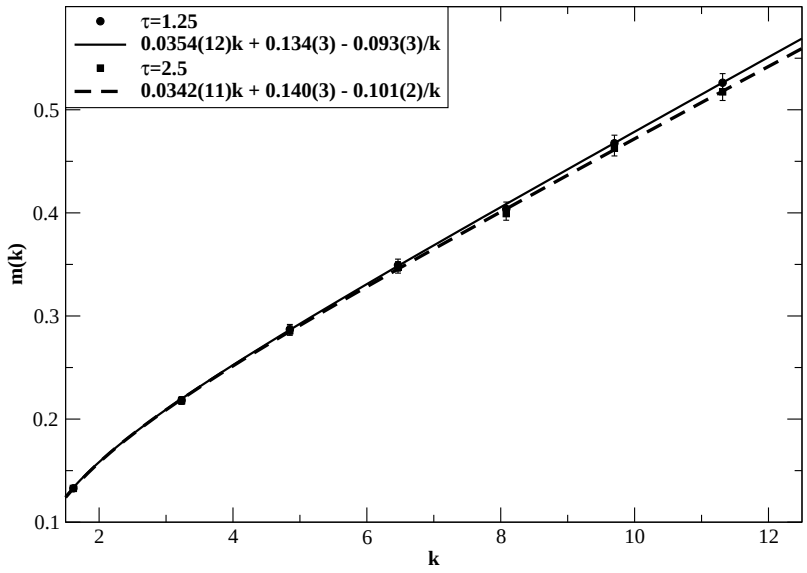

Figure 7: The ground state energy $m(k)$ as a function of k for two different values of the smearing parameter at $b = 0.8$.

be addressed. In addition, we also have to address finite volume effects since continuum reduction is valid only in the $N \to \infty$ limit.

We expect $m(k)$ to have a fixed limit as $N \to \infty$ at a fixed k, L, b and τ. Indeed, this is the case as shown in figure 8 where the results for $m(k)$ as a function of k are shown for $b = 0.8$ with $\tau = 2.5$ on 5^3 lattice. All three fit parameters are consistent within errors all the way from $N = 23$ to $N = 47$. The only glitch one sees is at $k \approx 8$. This corresponds to $K = kb_I = 5$, which is the linear extent of the lattice. One can argue that there are larger finite N effects at strong coupling for $K = L$. Since the fit of $m(k)$ involves several values of k, the larger effect at this particular value of k is diminished in the extraction of σb_I^2.

Since finite N effects can be ignored at $N = 47$, we also expect there to be no appreciable finite volume effects at this value of N. This point is illustrated in figure 9 where the result for $m(k)$ is plotted at $b = 0.6$ and $\tau = 2.5$ on 4^3 and 5^3 lattice. We used $b = 0.6$ for this comparison since we have to be in the confined phase on 4^3 lattice. Figure 9 shows that the two values of $m(k)$ at a fixed k are consistent with each other within errors. The same is the case for the fit parameter σb_I^2. This is not the case for c_1 and $c_0 b_I$, and this is probably due to a three parameter fit using only five data points. Sub-leading coefficients are expected to depend sensitively on the data points. Since we are primarily concerned with the value of the string tension in this paper and since all our results are based on data taken on 5^3, we expect the final result to be free of finite N and finite L errors.

6. Creutz ratio

It is natural to ask how the Creutz ratio [12],

$$\chi(K, J) = -\ln \frac{W(K, J)W(K-1, J-1)}{W(K, J-1)W(K-1, J)}, \tag{6.1}$$

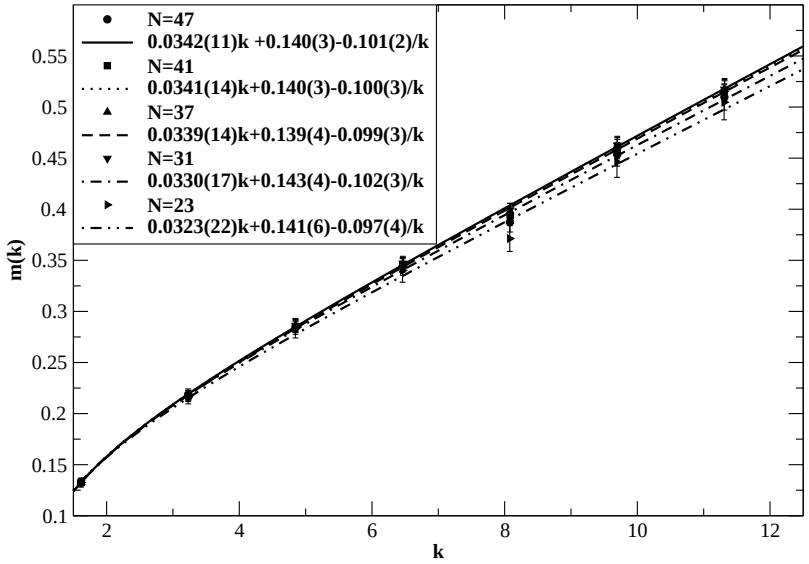

Figure 8: $= 0.8$.

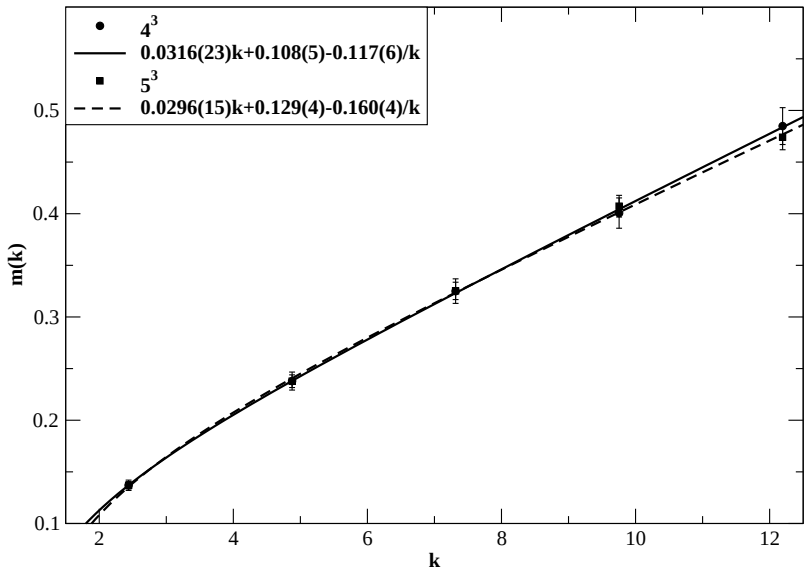

Figure 9: The ground state energy $m(k)$ as a function of k on two different lattices at $b = 0.8$.

performs as an observable from which to extract the string tension. If we were to use Creutz ratios, we would have smeared all links using all staples. But one can still ask how the Creutz ratio behaves with the asymmetrically smeared links. We show this for square loops ($J = K$) at $b = 0.8$ and $\tau = 2.5$ in figure 10. The solid lines show the estimate for the $\sqrt{\sigma}b_I$ as obtained from the analysis in this paper. There is no evidence for a plateau in the Creutz ratio in the range of k shown in figure 10. It is possible the situation would be different if we had smeared all links.

Each data point in figure 10 is obtained using only four different Wilson loops, i.e. four

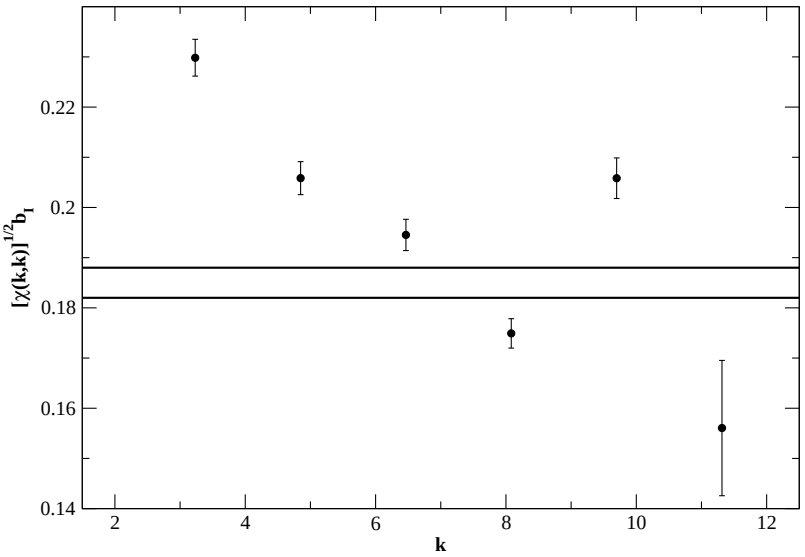

Figure 10: Behavior of the Creutz ratio for square loops at $b = 0.8$.

of the data points in figure 5. This is quite different from the analysis in this paper. Seven different Wilson loops in figure 5 are used to extract one $m(k)$ point in figure 2, and the loops used for different k form independent sets. Then the $m(k)$ are fit to determine the string tension. Both folded and unfolded loops contribute together. This is the main reason we succeeded in extracting the string tension using the range of Wilson loops considered here. To extract the string tension using Creutz ratios, larger loops and therefore larger statistics and possibly larger N would be needed.

7. Conclusions

We used Wilson loops with smeared space-like links and unsmeared time-like links to obtain an estimate for the string tension in the large N limit of three dimensional Yang-Mills theory. Invoking large N continuum reduction, we included Wilson loops larger than the size of the lattice. Since we used smeared space-like links, the Wilson loops for fixed length in space and varying length in time showed excellent agreement with a single exponential. The ground state energy so obtained was fit using three parameters to get an estimate for the string tension. The ground state energy exhibited short distance behavior at the shortest length used in the paper but large enough distances were used to get an estimate for the dimensionless string tension with small errors (Equation 1.3). These results validate the method of continuum reduction for calculating quantities based on the space-time dependence Wilson loops.

Acknowledgments

R.N. acknowledges partial support by the NSF under grant number PHY-055375.

References

[1] R. Narayanan and H. Neuberger, *Large-N reduction in continuum*, *Phys. Rev. Lett.* **91** (2003) 081601 [hep-lat/0303023].

[2] J. Kiskis, R. Narayanan and H. Neuberger, *Does the crossover from perturbative to nonperturbative physics in QCD become a phase transition at infinite N ?*, *Phys. Lett.* **B 574** (2003) 65 [hep-lat/0308033].

[3] R. Narayanan and H. Neuberger, *Chiral symmetry breaking at large-N_c*, *Nucl. Phys.* **B 696** (2004) 107 [hep-lat/0405025].

[4] R. Narayanan and H. Neuberger, *The quark mass dependence of the pion mass at infinite N*, *Phys. Lett.* **B 616** (2005) 76 [hep-lat/0503033].

[5] B. Bringoltz and M. Teper, *A precise calculation of the fundamental string tension in* SU(N) *gauge theories in* $2+1$ *dimensions*, *Phys. Lett.* **B 645** (2007) 383 [hep-th/0611286].

[6] D. Karabali, C.-j. Kim and V.P. Nair, *On the vacuum wave function and string tension of Yang-Mills theories in* $(2+1)$ *dimensions*, *Phys. Lett.* **B 434** (1998) 103 [hep-th/9804132].

[7] M.J. Teper, SU(N) *gauge theories in* $2+1$ *dimensions*, *Phys. Rev.* **D 59** (1999) 014512 [hep-lat/9804008].

[8] M. Lüscher, K. Symanzik and P. Weisz, *Anomalies of the free loop wave equation in the WKB approximation*, *Nucl. Phys.* **B 173** (1980) 365.

[9] P. de Forcrand, G. Schierholz, H. Schneider and M. Teper, *The string and its tension in* SU(3) *lattice gauge theory: towards definitive results*, *Phys. Lett.* **B 160** (1985) 137.

[10] F. Bursa and M. Teper, *Strong to weak coupling transitions of* SU(N) *gauge theories in* $2+1$ *dimensions*, *Phys. Rev.* **D 74** (2006) 125010 [hep-th/0511081].

[11] R. Narayanan, H. Neuberger and F. Reynoso, *Phases of three dimensional large-N QCD on a continuum torus*, *Phys. Lett.* **B 651** (2007) 246 [arXiv:0704.2591].

[12] M. Creutz, *Quarks, gluons and lattices*, Cambridge University Press, Cambridge U.K. (1983), pg. 169.

JHEP09(2008)080